Boundary layer on a circular cylinder in axial flow

S. P. Sawchuk and M. Zamir
Department of Applied Mathematics, University of Western Ontario, London, Ontario, Canada

Quasi-similar solutions are presented for the boundary layer on a circular cylinder in axial flow, using a Keller-Box numerical scheme to solve for velocity components rather than a stream function. The solutions extend earlier results considerably and cover a wide range of cylinder radii from very small (needle case) to very large (Blasius case). Velocity profiles, skin friction, and boundary-layer thickness parameters are presented and compared with earlier results. The results are given in sufficient detail to provide useful guidelines for engineering applications.

Keywords: boundary layer; viscous flow; cylinder

Introduction

Viscous flow along the outer surface of a circular cylinder in axial flow, despite its simple geometry, does not have a universal similarity solution of the boundary-layer type. The reason for this is that the space coordinates that must be used within the boundary layer are either x, y or x, r, where x is streamwise distance measured from the leading edge, and y and r are radial distances measured from the surface and from the axis of the cylinder, respectively. The first choice is appropriate when the boundary-layer thickness is small compared with the radius of the cylinder while the second is appropriate when that thickness is large. These two limits of the problem are sometimes referred to as the Blasius and needle limits, respectively. The limits arise not only when cylinders of extreme radii are considered, but when a cylinder of any given radius is considered along its full length. As the boundary layer develops in the streamwise direction and its thickness grows, both limits would usually prevail on the same cylinder.

More quantitatively these limits can be expressed in terms of the value of a nondimensional parameter

$$\xi = 4\left(\frac{x}{a}\right)^{1/2}\left(\frac{Ua}{\nu}\right)^{-1/2} \tag{1}$$

where U is the main stream velocity, a is the radius of the cylinder, and ν is the kinematic viscosity. As $\xi \to \infty$ the needle limit is approached and the flow becomes a function of x, r, while as $\xi \to 0$ the Blasius limit is approached and the flow becomes a function of x, y. The full range of the problem is thus described by $0 < \xi < \infty$.

Because of these difficulties there are no solutions at present that cover the full range of the problem. Seban and Bond[1] and Kelly[2] obtained series expansions for the velocity components and some integral properties of the boundary layer in the range $\xi \leqslant 1$. Glauert and Lighthill[3] and Stewartson[4] obtained asymptotic expansions of skin-friction and some integral properties, for $\xi \geqslant 200$. Jaffe and Okamura[5] obtained the same results numerically for $\xi \leqslant 40$, and Cebeci[6] and Cebeci and Smith,[7] using different numerical methods, produced results for $\xi \leqslant 64$.

Since heat transfer from the surface of the cylinder and the skin friction on it depend on the properties of this boundary layer, the accuracy with which these properties are known is important for engineering applications. In the absence of similarity, and hence the absence of a single solution from which data can be obtained, it would be difficult at present to produce estimates of heat transfer or skin friction on a given cylinder.

The purpose of this paper is to propose a method of solution that can deal in principle with the full range of this problem and to present results in the range $0 \leqslant \xi \leqslant 10^3$. The results are given in quasi-similar form and in sufficient detail to provide essential features of the boundary layer from which estimates of heat transfer and skin friction can be obtained on any cylinder within this wide range. The results also provide a useful framework in which to examine the accuracy and range of validity of other results now available, as well as fill the gaps between them. The method of solution consists of solving for velocity components (primitive variables) rather than a stream function, in a numerical Box scheme first introduced by Keller and Cebeci,[8] which we shall refer to as the Keller-Box method.

Equations

The equations governing the flow were first derived by Sowerby and Cooke[9] in the form

$$u\frac{\partial u}{\partial x} + v\frac{\partial u}{\partial r} = \nu\left(\frac{\partial^2 u}{\partial r^2} + \frac{1}{r}\frac{\partial u}{\partial r}\right) \tag{2}$$

$$\frac{\partial u}{\partial x} + \frac{\partial v}{\partial r} + \frac{v}{r} = 0 \tag{3}$$

with $u = v = 0$ at $r = a$ and $u \to U$ as $r \to \infty$ (4)

where u, v are velocity components in the axial and radial directions, respectively, and U is the mainstream velocity.

Address reprint requests to Dr. Zamir at the Department of Applied Mathematics, Engineering and Mathematical Sciences Building, University of Western Ontario, London, Ontario, N6A 5B9, Canada.

Received 4 June 1991; accepted 3 September 1991

These are essentially boundary-layer equations obtained from the full Navier-Stokes equations by making the usual boundary-layer assumptions, with one added assumption regarding the cylinder radius a. Sowerby and Cooke[9] assumed that a is at most of the same order as the boundary-layer thickness, and this would seem to restrict the validity of the equations to values of ξ near the needle limit of the problem. However, it turns out that the equations enjoy wider validity than this since the only two terms that contain r explicitly vanish as $r \to \infty$, and with appropriate scaling the equations reduce to Prandtl's two-dimensional boundary-layer equations.[10]

Method of solution

Writing

$$\eta = \left(\frac{U}{2\nu x}\right)^{1/2} y, \quad \text{and} \quad H = 1 + \frac{\xi}{2\sqrt{2}}\eta \tag{5}$$

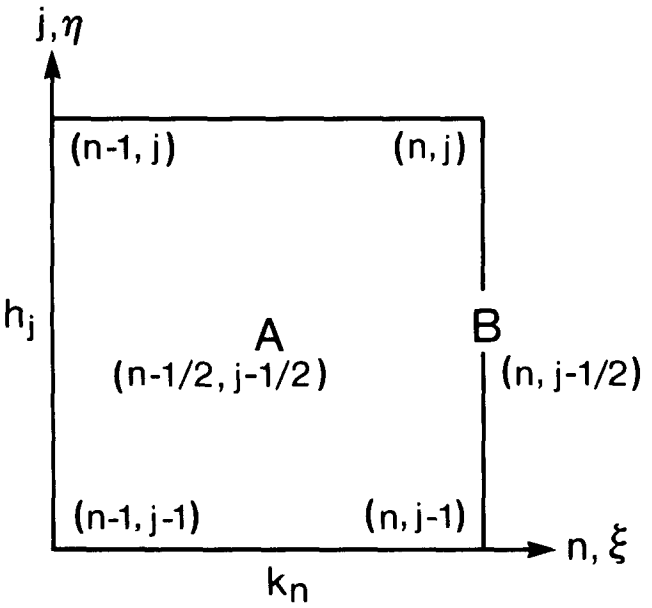

Figure 1 Box used for discretization of Equations 7 and 8 (centered at A) and Equation 6 (centered at B)

$$P = u/U, \quad Q = v/U, \quad \tilde{Q} = H\left(\eta P - \frac{R_a \xi}{2\sqrt{2}} Q\right)$$

and

$$T = \frac{\partial P}{\partial \eta} \tag{6}$$

the governing equations are transformed to

$$(HT)_\eta + \tilde{Q}T = \xi H P P_\xi \tag{7}$$

$$\tilde{Q}_\eta - (2H - 1)P = \xi H P_\xi \tag{8}$$

with boundary conditions

$$P = \tilde{Q} = Q = 0 \quad \text{at } \eta = 0 \quad \text{and} \quad P \to 1 \quad \text{as } \eta \to \infty \tag{9}$$

Equations 6–8 are now discretized over a box centered at $(j - 1/2, n - 1/2)$, as shown in Figure 1, following a second-order method by Keller and Cebeci.[8] The resulting discretized equations are given by

$$\begin{aligned} &H^j T^j - H^{j-1} T^{j-1} + \frac{h_j}{4}(\tilde{Q}^j + \tilde{Q}^{j-1})(T^j + T^{j-1}) \\ &\quad - \xi_{n-1/2} H^{j-1/2}_{n-1/2} \frac{h_j}{4k_n}(P^j + P^{j-1})^2 \\ &= H^{j-1}_{n-1} T^{j-1}_{n-1} \\ &\quad - H^j_{n-1} T^j_{n-1} - \frac{h_j}{4}(\tilde{Q}^j_{n-1} + \tilde{Q}^{j-1}_{n-1})(T^j_{n-1} + T^{j-1}_{n-1}) \\ &\quad - \xi_{n-1/2} H^{j-1/2}_{n-1/2} \frac{h_j}{4k_n}(P^j_{n-1} + P^{j-1}_{n-1})^2 \end{aligned} \tag{10}$$

and

$$\begin{aligned} &\tilde{Q}^j - \tilde{Q}^{j-1} - \frac{h_j}{2}\left\{H^j_n + H^{j-1}_n - 1 \right. \\ &\quad \left. + \frac{(\xi_n + \xi_{n-1})}{4k_n}(H^j_n + H^{j-1}_n + H^j_{n-1} + H^{j-1}_{n-1})\right\} \\ &\quad \times (P^j + P^{j-1}) \\ &= \frac{h_j}{2}\left\{H^j_{n-1} + H^{j-1}_{n-1} - 1 - \frac{(\xi_n + \xi_{n-1})}{4k_n}\right. \\ &\quad \left. \times (H^j_n + H^{j-1}_n + H^j_{n-1} + H^{j-1}_{n-1})\right\} \\ &\quad \times (P^j_{n-1} + P^{j-1}_{n-1}) + \tilde{Q}^{j-1}_{n-1} - \tilde{Q}^j_{n-1}, \end{aligned} \tag{11}$$

Notation

a	Cylinder radius
u, v	Velocity components in the streamwise and radial directions, respectively
U	Constant mainstream velocity in axial direction
r, y	Radial distances measured from the axis and from the surface of cylinder, respectively
x	Streamwise distance measured from the leading edge
P	$= u/U$
Q	$= v/U$
R_a	Reynolds number $= Ua/\nu$
T	$= \partial P/\partial \eta$
T_0	$= \left(\frac{\partial u}{\partial \eta}\right)_{y=0} = \frac{\xi a}{2\sqrt{2}}\left(\frac{\partial u}{\partial y}\right)_{y=0}$

Greek symbols

ξ	$= 4\left(\frac{x}{a}\right)^{1/2}\left(\frac{Ua}{\nu}\right)^{-1/2}$
η	$= (U/2\nu x)^{1/2} y$
ϕ_1	$= (U/\nu a^2 x)^{1/2} \int_a^\infty \left(1 - \frac{u}{U}\right) r\, dr$
ϕ_2	$= (U/\nu a^2 x)^{1/2} \int_a^\infty \frac{u}{U}\left(1 - \frac{u}{U}\right) r\, dr$

with

$$P^j - P^{j-1} - \frac{h_j}{2}(T^j + T^{j-1}) = 0 \tag{12}$$

where

$$H_n^j = 1 + \frac{\xi_n}{2\sqrt{2}}\eta^j \tag{13}$$

$$H_{n-1/2}^{j-1/2} = \frac{1}{4}(H_n^j + H_n^{j-1} + H_{n-1}^j + H_{n-1}^{j-1}) = 1 + \frac{\xi_{n-1/2}}{2\sqrt{2}}\eta^{j-1/2} \tag{14}$$

and

$$P_n^1 = \tilde{Q}_n^1 = 0 \quad \text{and} \quad P_n^J = 1, \quad \text{for all } n \tag{15}$$

noting that

$$1 \leqslant j \leqslant J \quad \text{and} \quad 1 \leqslant n \leqslant N \tag{16}$$

Introducing the iterates

$$P_{(i+1)} = P_{(i)} + \delta P_{(i)}, \quad \tilde{Q}_{(i+1)} = \tilde{Q}_{(i)} + \delta\tilde{Q}_{(i)} \quad \text{and} \quad T_{(i+1)} = T_{(i)} + \delta T_{(i)} \tag{17}$$

Newton's method is applied to the discretized equations to solve for the linear perturbation terms by an iteration procedure in which quadratic and higher order terms are neglected. It was shown by Keller[11] that cancellation errors are reduced in this way, as compared with solving for the absolute quantities during iteration. A block tridiagonal factorization procedure is used to solve the resulting system of equations.[10]

An initial linear velocity profile is used to start the iteration at $\xi = 0$. At subsequent values of $\xi > 0$ the profile calculated at the previous step is used as initial profile. The iteration at each step in ξ is concluded with a convergence test in which $\delta T(0)$ is used as a measure of iteration error. The entire procedure is concluded when a desired value of ξ has been reached. Results could thus be continued in principle to any value of ξ.

At each step in ξ a test is carried out to ensure that the outer boundary condition is satisfied asymptotically. This is done by requiring that the value of $T(\eta_\infty)$ has reached zero to some specified tolerance. The use of similarity coordinates ξ and η was found to simplify this process considerably by causing this condition to be satisfied at about the same grid location.

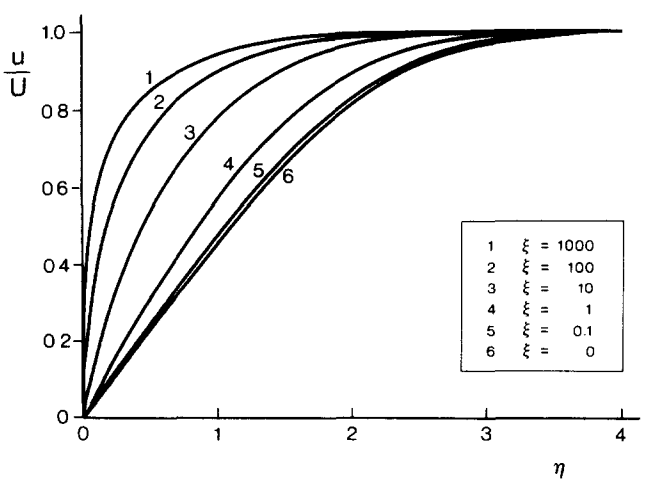

Figure 2 Profiles of axial velocity components in the boundary layer on cylinders with radii ranging from very small ($\xi \to \infty$) to very large ($\xi \to 0$)

Numerical solutions were obtained using three different mesh sizes, then Richardson extrapolation was used to increase the accuracy of the results from second to fourth order. It was shown by Keller and Cebeci[8] and Keller[11,12] that this is justified since errors in the numerical solution have asymptotic expansions in powers of the squares of the mesh size.

Results and discussion

Results are presented for values of ξ in the range 0–1000. This extends earlier results considerably and well covers the grounds between cylinders of very large radii (Blasius limit) to those of very small radii (needle limit).

Profiles of axial and radial velocity components (u, v) are shown in Figures 2 and 3, respectively. The nonsimilar nature of the flow is clearly evident from the dependence of these profiles on the value of ξ. Similarity of velocity profiles is approached only toward the two limits of the problem: as $\xi \to 0$ they collapse onto the Blasius profile and as $\xi \to \infty$ they collapse onto the square profile that prevails in the needle case, as illustrated in Figures 2 and 3. By comparison with the Blasius profile (no. 6 in Figures 2 and 3) it is seen that the boundary

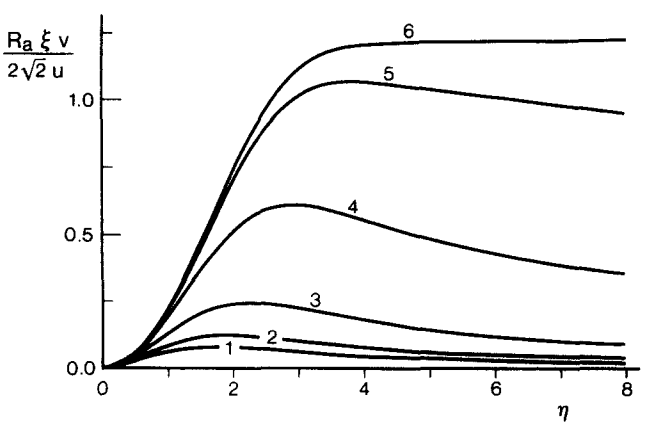

Figure 3 Profiles of radial velocity components. Legend and remaining caption as for Figure 2

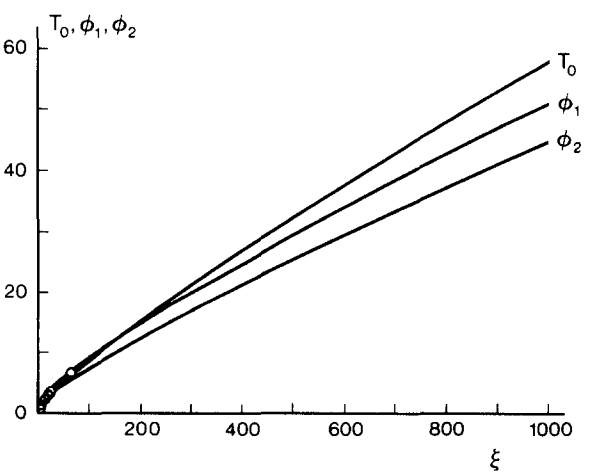

Figure 4 Skin friction (T_0), displacement thickness (ϕ_1), and momentum thickness (ϕ_2) parameters, as defined by Equations 18–20 for different values of ξ. The curves represent current results while the data points are from Cebeci and Smith[7]

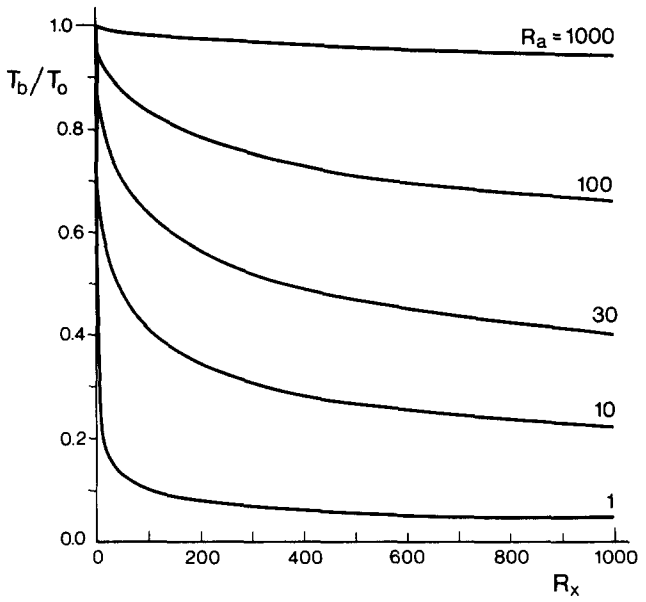

Figure 5 Ratio of skin friction on a flat plate (T_b) to that on a cylinder (T_0) in terms of the Reynolds numbers R_a and R_x based on cylinder radius and streamwise distance, respectively

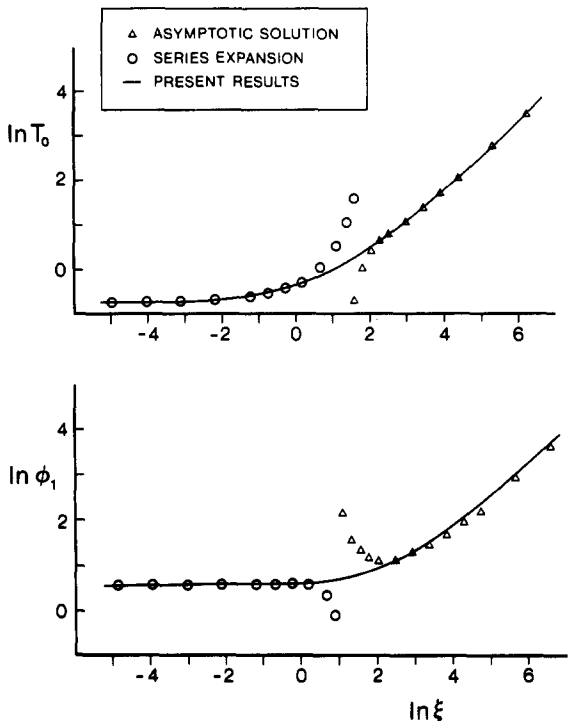

Figure 6 Comparison of present results for skin friction (T_0) and displacement thickness (ϕ_1) with the asymptotic solution[3] and a series expansion[1,2,13] for small ξ

layer on a cylinder is typically thinner than the Blasius boundary layer on a flat plate and contains smaller radial velocities.

Skin friction and boundary-layer thickness parameters, T_0, ϕ_1, ϕ_2, as defined below, are shown in Figure 4, again in the range $0 \leqslant \xi \leqslant 1000$.

$$T_0 = \frac{\xi a}{2\sqrt{2}}\left(\frac{\partial u}{\partial y}\right)_{y=0} \tag{18}$$

$$\phi_1 = (U/va^2x)^{1/2}\int_a^\infty \left(1 - \frac{u}{U}\right) r\, dr \tag{19}$$

$$\phi_2 = (U/va^2x)^{1/2}\int_a^\infty \frac{u}{U}\left(1 - \frac{u}{U}\right) r\, dr \tag{20}$$

Since the boundary layer on a cylinder is generally thinner than that on a flat plate, the skin friction would be higher, as shown in Figure 5. Each curve in that figure represents a cylinder of a given radius, more specifically a Reynolds number R_a based on that radius. At a given point x on the cylinder, the skin friction is given in terms of the Reynolds number R_x based on x. For $R_a = 1.0$, for example, the skin friction on the cylinder (T_0) is about 20 times higher than it is on a flat plate (T_b) at $R_x = 1000$, which corresponds to a distance of 1000 cylinder radii from the leading edge. Along this particular cylinder the ratio T_b/T_0 decreases from 1.0 at the leading edge to about 0.1 at $R_x = 100$ and 0.05 at $R_x = 1000$.

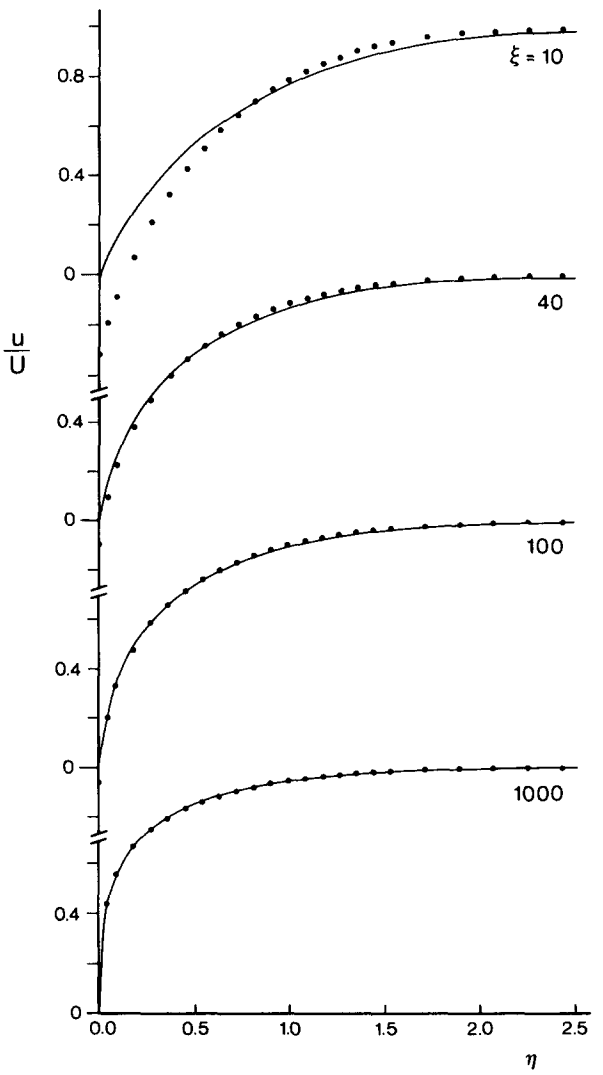

Figure 7 Comparison of profiles of axial velocity obtained from the present results (---) with those obtained from the asymptotic solution (· · ·)

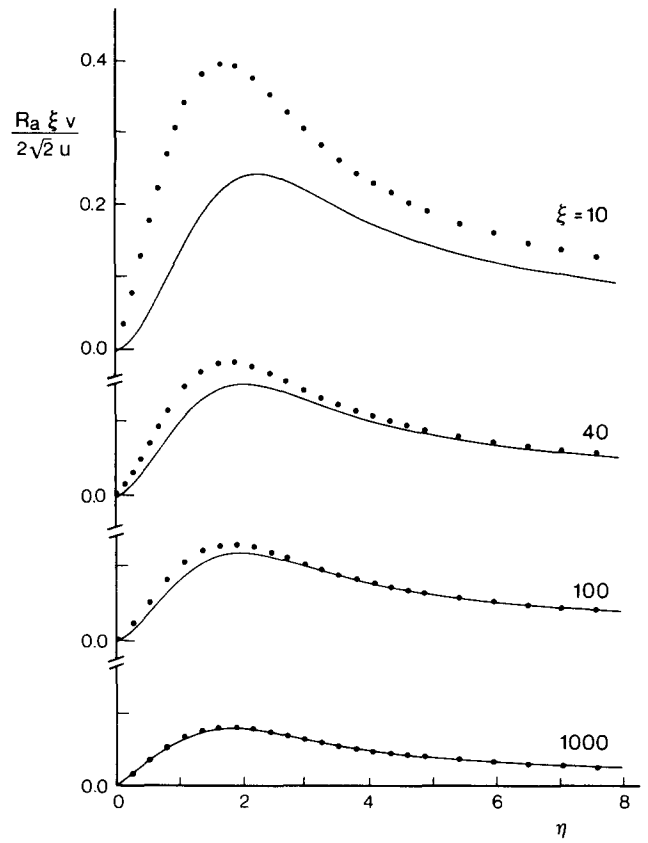

Figure 8 Comparison of profiles of radial velocity obtained from the present results (---) with those obtained from the asymptotic solution (· · ·)

Comparison of present results for skin friction with those of Cebeci and Smith[7] is shown in Figure 4. The agreement is good in the small range of ξ for which the latter were obtained. Comparisons with the asymptotic solution[3] and a series expansion[1,2,13] for small ξ are shown in Figure 6. It is seen that the asymptotic solution may yield reasonably accurate estimates of skin friction for values of ξ as low as 10, while the series expansion may do so for values of ξ as high as 1.0. Between these two values of ξ there is a pronounced gap where both become increasingly invalid. This gap is in fact much wider than it appears, however, when velocity profiles are considered and when numerical values of the results are examined more closely.

Comparisons of actual velocity profiles are shown in Figures 7 and 8 where finer differences can be clearly observed. At $\xi = 10$, for example, where the asymptotic solution produces a reasonably accurate value of skin friction, it produces fairly inaccurate values of the velocity components (u, v), particularly near the surface. This discrepancy is much larger for v than it is for u, and it is still present at values of ξ as high as 1000, although it is then very small.

In summary, Figures 2–5 provide data in quasi-similar form that document the properties of the boundary layer on a circular cylinder in axial flow for a wide range of cylinder radii. The data provide the basis for estimates of heat transfer from the surface of a given cylinder or of the skin friction on it.

Acknowledgments

This work was supported by the Natural Sciences and Engineering Research Council of Canada. We acknowledge with gratitude helpful discussions with Professor A. D. Young of the University of London, Professor N. Riley of the University of East Anglia, and Dr. S. E. Camiletti of Kings College, London (Canada).

References

1 Seban, R. A. and Bond, R. Skin friction and heat transfer characteristics of a laminar boundary layer on a circular cylinder in axial incompressible flow. *J. Aero. Sci.*, 1951, **18**, 671–675

2 Kelly, H. R. A note on the laminar boundary layer on a circular cylinder in axial incompressible flow. *J. Aero. Sci.*, 1954, **21**, 634

3 Glauert, M. B. and Lighthill, M. J. The axisymmetric boundary layer on a long thin cylinder. *Proc. R. Soc. Lond.*, 1954, **230**, 189–203

4 Stewartson, K. The asymptotic boundary layer on a circular cylinder in axial incompressible flow. *Quart. Appl. Math.*, 1955, **13**, 113–122

5 Jaffe, N. A. and Okamura, T. T. The transverse curvature effect of the incompressible boundary layer for longitudinal flow over a cylinder. *Z. Angew. Math. Phys.*, 1968, **19**, 564–574

6 Cebeci, T. Laminar and turbulent incompressible boundary layers on slender bodies of revolution in axial flow. *J. Basic Eng.*, 1970, **92**, 545–553

7 Cebeci, T. and Smith, A. M. O. *Analysis of Turbulent Boundary Layers*. Academic Press, New York, 1974

8 Keller, H. B. and Cebeci, T. Accurate numerical methods for boundary layer flows I: Two-dimensional laminar flows. *Proc. 2nd Int. Conf. Numer. Meth. Fluid Dyn.*, Berkeley, CA, 1970, *Lect. Notes Phys.*, 1971, **8**, 92–100

9 Sowerby, L. and Cooke, J. C. The flow of fluid along corners and edges. *Quart. J. Mech. Appl. Math.*, 1953, **6**, 53–54

10 Sawchuk, S. P. Circular cylinder in axial flow. Ph.D. thesis, University of Western Ontario, Canada, 1990

11 Keller, H. B. Numerical methods in boundary-layer theory. *Ann. Rev. Fluid Mech.*, 1978, **10**, 417–433

12 Keller, H. B. Some computational problems in boundary-layer flows. *Proc. 4th Int. Conf. Numer. Meth. Fluid Dyn.*, Boulder, CO, 1974, *Lect. Notes Phys.*, 1975, **35**, 1–21

13 Sawchuk, S. P. Boundary layer on a circular cylinder in axial flow. M.Sc. thesis, University of Western Ontario, Canada, 1985